Journal of Electrical Engineering, Vol. 74, No. 4, 2023, pp. 267-276

sciendo
PAPER

Harmonic reduction of grid-connected multilevel inverters using modulation of variable frequency carriers

Quang-Tho Tran

Multilevel three-phase inverters are increasingly popular due to their ability to generate high-quality output voltage with harmonic distortion lower than traditional inverters. They are used in various applications, including grid-connected renewable energy systems, motor drives, and power transmission systems, to improve efficiency and reduce costs. The control quality of grid-connected multilevel inverters depends on various factors such as the modulation technique, switching frequency, and control strategy. A good control system can achieve a balance between output current harmonics and switching losses, improving the efficiency and performance of the inverter. This paper suggests a technique for reducing current harmonics of grid-connected multilevel three-phase inverters using variable frequency carriers, without any corresponding increase of the number of switching commutations. The effectiveness of the suggested method has been confirmed through simulation results, which were compared to those obtained from the method of phase opposite disposition modulation using fixed frequency carriers.

Keywords: grid-connected three-phase multilevel inverter, common mode voltage, modulation, number of switching commutations, total harmonic distortion

1. Introduction

Multilevel three-phase inverters have become popular in recent years due to their ability to provide high-quality output voltage with reduced harmonic distortion. They are suitable for various applications, including renewable energy systems, electric vehicles, and industrial automation, where efficient and reliable power conversion is crucial [1-3]. The multilevel three-phase inverters have also gained attention in grid-connected applications, where they help reduce power losses and increase system efficiency. Their popularity is expected to continue to grow as the demand for energy-efficient and clean energy solutions increases [1,2], [4-7]. Additionally, ongoing research and development in the field are expected to lead to further improvements in performance and cost-effectiveness.

The power quality of grid-connected multilevel inverters highly depends on the quality of control mechanisms used to regulate the output voltage and modulation methods. Moreover, current controllers, phase-lock loop (PLL), and quality of dc voltage source also significantly affect the output voltage quality of inverters. Especially, the high magnitude of common mode voltage (CMV) adversely affects the power quality of the grid-connected inverter systems and generates leakage current and harmonics into the grid [8].

There are many methods for modulating multilevel inverters. They basically include pulse-width modulation (PWM) and space vector modulation (SVM) [9,10]. To reduce the magnitude of CMV, several methods can be employed. One method is to use symmetrically interleaved PWM, which can cancel out the CMV by generating equal and opposite voltage vectors in the two half-bridges of the inverter. Another method is to use PWM techniques with modified third harmonic injection and max-min strategy, which can reduce CMV. Additionally, multilevel inverters can benefit from using active and passive filtering techniques, such as common mode chokes or common mode capacitors, which can reduce the CMV and limit the electromagnetic interference emissions. Most methods of space vector modulation (SVM) for multilevel inverters use a combination of multiple carrier waves and vector addition to generate the output voltage waveform. This technique provides good harmonic reduction and precise control over the output voltage waveform. However, the higher the number of levels is, the more complex the SVM is when compared with the PWM [11] and the phase-shifted carrier modulation to generate multilevel output voltage [12,13]. In methods such as phase disposition (PD), phase opposite disposition (POD), and alternate phase opposite disposition (APOD) [14,15], each with its advantages and disadvantages, the POD and APOD can offer the magnitude of CMV lower than that of the PD. These methods use the carriers with fixed frequency to modulate inverters. These carriers do not contain any information on the modulated signal. In addition, most of these modulation methods have not considered the number of switching commutations and application for grid-connected inverters [16,17]. Advanced modulation techniques can significantly improve the power quality of multilevel inverters, making them a suitable option for various applications. However, the implementation of advanced modulation techniques requires a sophisticated control system, which can increase the cost and complexity of the system.

Frequency modulation of carriers has numerous applications in communication systems, particularly in radio broadcasting and mobile communication systems. Additionally, this variable frequency carrier (VFC) is used in radar systems to measure the range and speed of objects, and in satellite communication systems for transmitting signals over long distances. By using VFCs, it is possible to achieve reliable and high-quality communication in a variety of applications. The ability to spread the spectrum

Faculty of Electrical and Electronics Engineering, HCMC University of Technology and Education, Vietnam
thotq@hcmute.edu.vn

https://doi.org/10.2478/jee-2023-0033, Print (till 2015) ISSN 1335-3632, On-line ISSN 1339-309X

over a wide range is also an advantage of these carriers [18]. However, in the grid-connected multilevel three-phase inverters, the VFC technique has not been used for modulating inverters.

This paper proposes a modulation method for the grid-connected multilevel three-phase inverters using the VFC technique. In this technique, the frequency of carriers varies based on the control signal. These carriers are known as frequency modulation carriers, which are highly effective in replicating control signal information. The adaptive carrier frequency variation based on the control signal amplitude can aid in producing the control signal at the inverter's output. Moreover, low frequency carriers can also improve the power quality of the inverter output voltage. A system of grid-connected cascaded 5-level 3-phase inverter is described in Section 2. The POD method using the fixed frequency carriers is also presented in Section 2. The approach of VFC method is presented in Section 3. The results of the POD method and the VFC technique are also shown in Section 4 with different values of reference powers. The performance of the VFC method is summarized in Section 5 when comparing the results of the POD with those of the VFC technique.

2. Grid-connected three-phase inverter

The structure of a grid-connected 5-level three-phase inverter system is shown in Fig. 1. This essential structure includes a PLL, a block of reference current calculation, current controller, and POD modulation. This system uses the current control method in the synchronous rotating frame (SRF). Therefore, the current and voltage quantities such as I_d, I_q, V_d, and V_q, in this frame are transformed by basing on the phase angle θ estimated by the PLL. Then, the reference currents injected into the grid in the SRF, $I_{d\text{-ref}}$ and $I_{q\text{-ref}}$, are calculated as shown in Eqn. (1) according to the reference powers, P_{ref} and Q_{ref}.

$$\begin{bmatrix} I_{d\text{-ref}} \\ I_{q\text{-ref}} \end{bmatrix} = \frac{(2/3)}{V_d^2 + V_q^2} \begin{bmatrix} V_d & -V_q \\ V_q & V_d \end{bmatrix} \begin{bmatrix} P_{ref} \\ Q_{ref} \end{bmatrix} \tag{1}$$

The current controller in the grid-connected inverters regulates the currents flowing into the grid to meet the reference power requirements. The current controller typically uses a proportional-integral (PI) control algorithm that adjusts the output voltage of the inverter to maintain the current at the desired reference value. These current controllers use the errors between the reference currents and the measured ones to regulate the reference voltages, $V_{d\text{-ref}}$ and $V_{q\text{-ref}}$. Then, these voltages are transformed to the reference phase voltages, $V_{ref\text{-}abc}$. The POD modulation uses these phase voltages as the inputs to modulate the inverter.

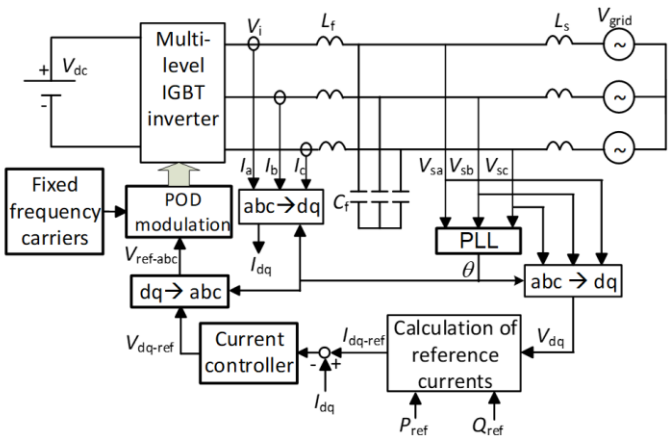

Fig. 1. Structure of grid-connected multilevel inverter system

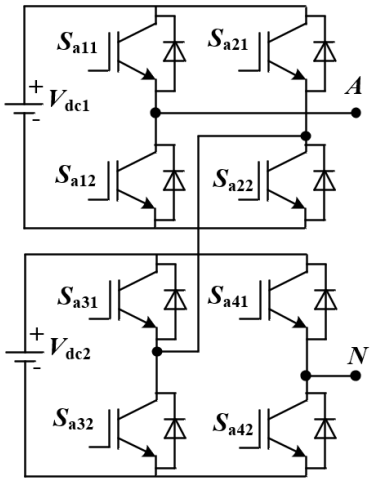

Fig. 2. Main circuit of phase A

The main circuit of one phase shown in Fig. 2 consists of two H-bridges using IGBT switches. Here, each arm has a top switch S_{xj1} and a bottom switch S_{xj2} (j=1÷4). Five levels of each phase of output voltage are shown in Table 1 and depend on the outputs S_{xj} of control diagram in Fig. 3. In this control diagram, R_x and L_x are the two components of the voltage G(t), ($x = a, b, c$). Here, G(t) is a signal normalized to the inverter levels defined in Eqn. (2). The level L_x ($0 \le L_x \le n-2$) is the integer of the signal G(t) and calculated by Eqn. (3). R_x ($0 \le R_x \le 1$) is the difference of the subtraction between G(t) and L_x, ($x = a, b, c$).

$$G(t) = (V_{r\text{-}abc} + 1)\frac{n-1}{2} \tag{2}$$

$$L_x = \begin{cases} n-2, \text{ if } G(t) \ge n-2 \\ \text{fix}\,(G(t)), \text{otherwise} \end{cases} \tag{3}$$

Table 1. Switching states of switches in phase A

n	S_{a11}	S_{a21}	S_{a31}	S_{a41}	Output voltage
1	0	1	0	1	$-2V_{dc}$
2	0	1	0	0	$-V_{dc}$
3	0	0	0	0	0
4	1	0	0	0	$+V_{dc}$
5	1	0	1	0	$+2V_{dc}$

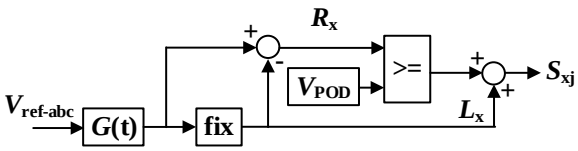

Fig. 3. General control diagram of inverter

POD is a commonly used method for modulating the output voltage of multilevel inverters in power electronics applications. The POD method involves arranging the switches in a multilevel inverter in a specific pattern to achieve the desired output voltage waveform. In the POD method, the adjacent switches in each leg of the inverter are turned on and off in opposite phases, resulting in a staircase waveform with reduced harmonic distortion. One advantage of the POD method is its simplicity and ease of implementation compared to other modulation techniques. The POD modulation using carriers with the fixed frequency for a 5-level inverter is also shown in Fig. 4. Where the control signal G(t) has a fundamental frequency of 50 (Hz), and the carriers have a frequency of 2 (kHz). The POD method gives the common mode voltage CMV of V_{dc}/3.

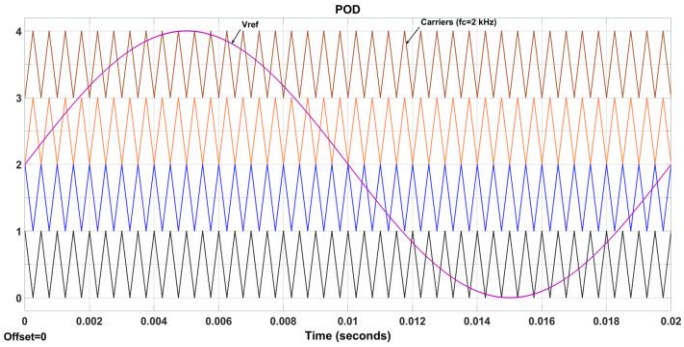

Fig. 4. POD modulation method

3. Proposed technique

In the proposed method, the carriers are used for modulating inverters having variable frequency. When the control signal has a sinusoidal form and described as

$$v_r(t) = V_{max}\sin(\omega_m t), \tag{4}$$

where V_{max} is the magnitude of the control signal. Using the control signal $v_r(t)$ to vary the frequency of $v_f(t)$ will obtain the frequency modulated carrier. According to the theory of modulation, v_f(t) will be defined as follows:

$$v_f(t) = F_{max}\cos[\omega_c t + \Delta\omega \int v_r(t)\mathrm{d}t], \tag{5}$$

where $\Delta\omega$ is a difference between the instantaneous angular frequency compared with the angular frequency of carrier ω_c. Then, Eqn. (5) can be rewritten as

$$v_{fc}(t) = F_{max}\cos[\omega_c t + M_F\Delta\omega \int v_r(t)\mathrm{d}t], \tag{6}$$

where M_F is frequency modulation index defined as (7). F_{max} is the magnitude of this signal.

$$M_F = \frac{\Delta\omega}{\omega_m} \tag{7}$$

Then, the carrier after frequency modulation will be as follows.

$$C_f(t) = \frac{2\arcsin(v_{fc}(t))}{\pi} \tag{8}$$

$$C_{VF} = \frac{C_f(t)+\max(C_f(t))}{\max(C_f(t))+\min(C_f(t))} \tag{9}$$

This carrier can also be rewritten as (9) after normalization. Varying the value of M_F and ω_c, we can obtain various carriers. The frequency modulated carriers are illustrated in Fig. 5 when the fundamental frequency of the control signal f_m is 50 (Hz), M_F as 10, and ω_c as 2000π (rad/s).

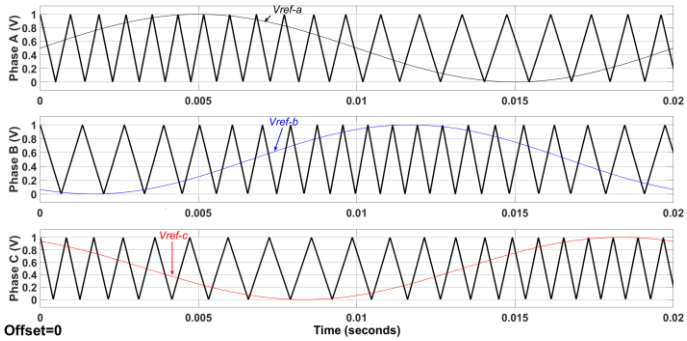

Fig. 5. Variable frequency carriers with ω_m =100π (rad/s); ω_c =2000π (rad/s) and M_F =10

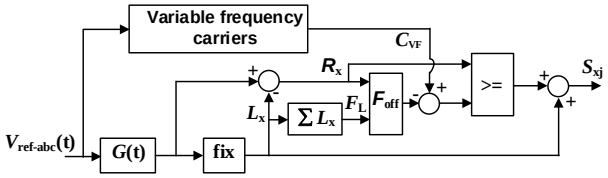

Fig. 6. Proposed control diagram using variable frequency carriers.

The inverter control principle of the proposed method is shown in Fig. 6. Where the variable frequency carrier is used for comparing with the signal R_x. In addition, an offset function in [19], F_{off} is also used to subtract from the carrier and defined as given in Eqn. (10). Here, F_L is the sum of L_x, (x=a, b, c).

$$F_{\text{off}} = \begin{cases} 1-\max(R_x) & \text{if } F_L = \frac{3(n-1)}{2} - 2 \\ -\min(R_x) & \text{if } F_L = \frac{3(n-1)}{2} - 1 \\ 0 & \text{otherwise} \end{cases} \quad (10)$$

4. Results and discussion

Table 2. System parameters

Parameter	Symbol	Value
Grid source voltage	V_g	3×380 (V)
Grid source frequency	f_m	50 (Hz)
Resistor of the grid source	R_s	0.01 (Ω)
Inductor of the grid source	L_s	0.1 (mH)
Resistor of filter at the inverter side	R_i	0.01 (Ω)
Inductor of filter at the inverter side	L_i	3.5 (mH)
Capacitor of filter	C_f	1 (mF)
DC voltage	V_{dc}	180 (V)
Coefficients of PI current controller	k_p, k_i	0.15, 20
Sample time of current controller	T_s	0.0001 (s)
Fixed frequency of carrier	f_{car}	2 (kHz)
Modulation index	M_F	3.4
Integral gain of (8)	k	7
Angular frequency of modulated carrier	ω_c	5000π (rad/s)
Magnitude of signal in (6)	F_{max}	1 (V)

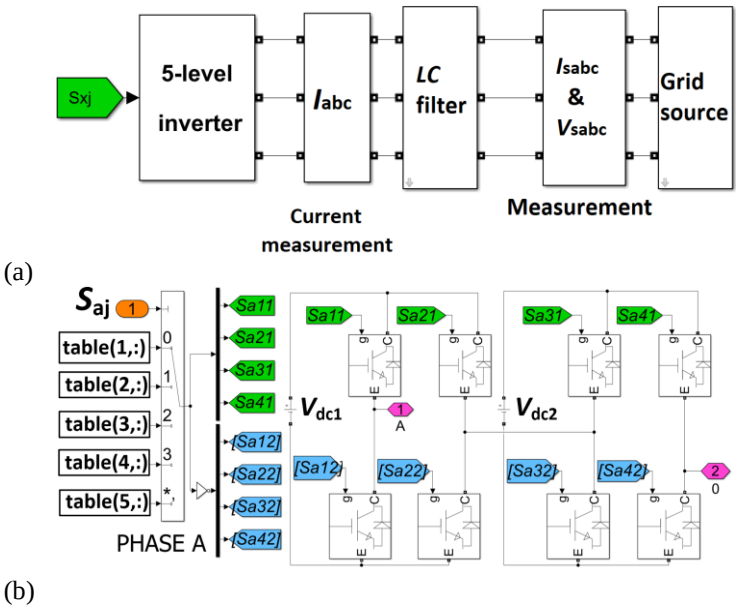

Fig. 7. Simulation model of (a) – system main circuit and (b) - structure of PWM output S_{aj} of main circuit of phase A

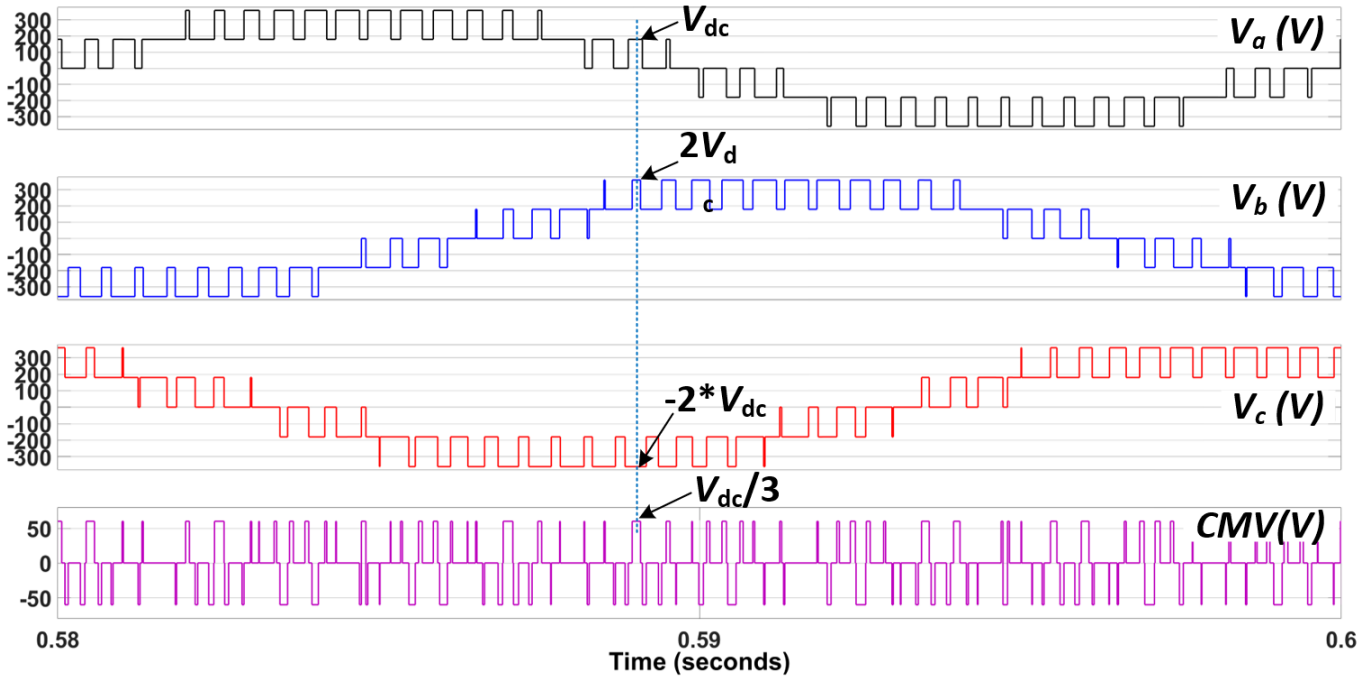

(a)

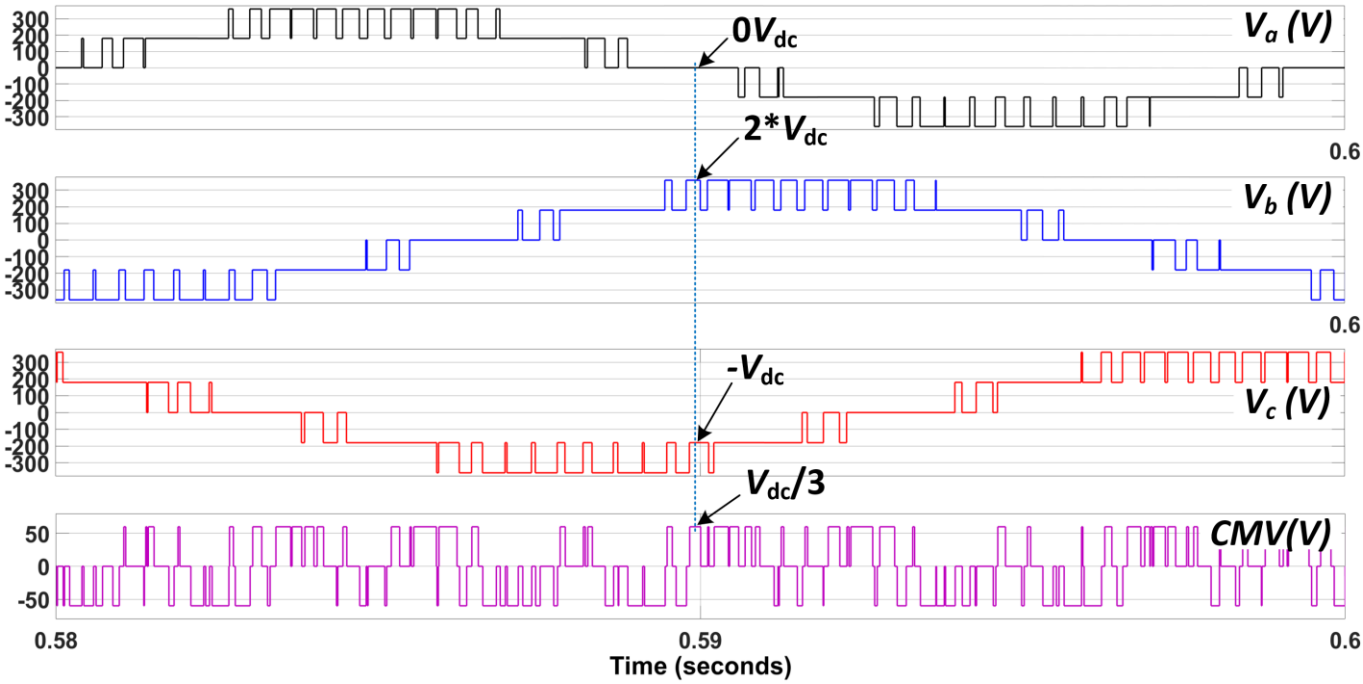

(b)

Fig. 8. Waveforms of phase voltages and common mode voltages zoomed in one fundamental period from 0.58-0.6 s: (a) POD method and (b) proposed method.

The simulation model of the grid-connected cascaded 5-level three-phase inverter is shown in Fig. 7 using software Matlab®/Simulink®. The system parameters are also presented in Table 2. There are three intervals of time that are surveyed in this system. The time of each interval is 0.3 (s). In the first interval, 0-0.3 (s), the reference active power P_{ref} is 20 (kW), the reference reactive power Q_{ref} is as 0.0 (Var). In the second interval, 0.3-0.6 (s), P_{ref} is stepped down to 10 (kW) whilst Q_{ref} is still as 0.0 (Var). In the final one, 0.6-0.9 (s), P_{ref} is stepped from 10 (kW) down to 0.0 (kW) while Q_{ref} is stepped from 0.0 (Var) up to 20 (kVar).

The surveyed results are shown in Figs. 8-13. The typical waveforms of phase voltages and CMV are shown in Fig. 8. These voltage waveforms are taken at the outputs of the inverter before filtering. These waveforms have shown that the number of switching commutations of the POD method as 42 in Fig. 8(a) is higher than that of the proposed method as 39 in Fig. 8(b) in one fundamental period. In addition, the CMV magnitude of the POD method in Fig. 8(a) as $V_{dc}/3$, calculated by an average sum of three phase voltage magnitudes at any moment, is equal to that of the proposed method in Fig. 8(b).

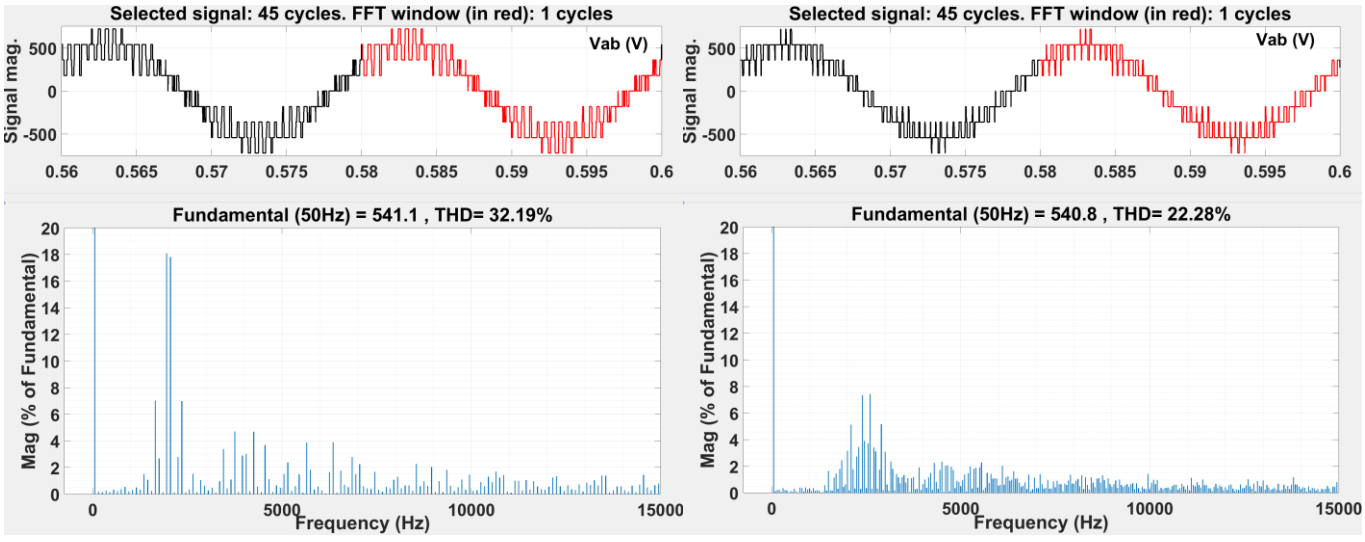

(a) (b)

Fig. 9. Line-line voltage spectra and THD values: (a) - of POD method and (b) - proposed method

The total harmonic distortion (THD) value of the line-line voltage, V_{ab} in Fig. 9(a) as 32.19% of the POD method, is higher than that of the proposed method as 22.28% in Fig. 9(b). Moreover, the spectra of the line-line voltages have also shown that the highest magnitude near the frequency of 2 (kHz) in Fig. 9(a) of the POD method is higher than 18% whilst that of the proposed

method in Fig. 9(b) is lower than 7.5%. Thus, the ability of spectrum spread of the proposed method helps reduce the highest magnitude of individual harmonic. This affects the spectrum spread of phase currents. In addition, the three-phase current waveforms injected into the grid of the two methods are also shown in Fig. 10. These waveforms are magnified in the last fundamental periods, 0.28-0.3 (s), 0.58-0.6 (s), and 0.88-0.9 (s) of the surveyed intervals correspondingly. The waveforms in Figs. 10(a)-(c) have showed that the current ripples of the POD method are higher than those of the proposed method in Figs. 10(d)-(f). These lead to reducing the harmonics of phase currents.

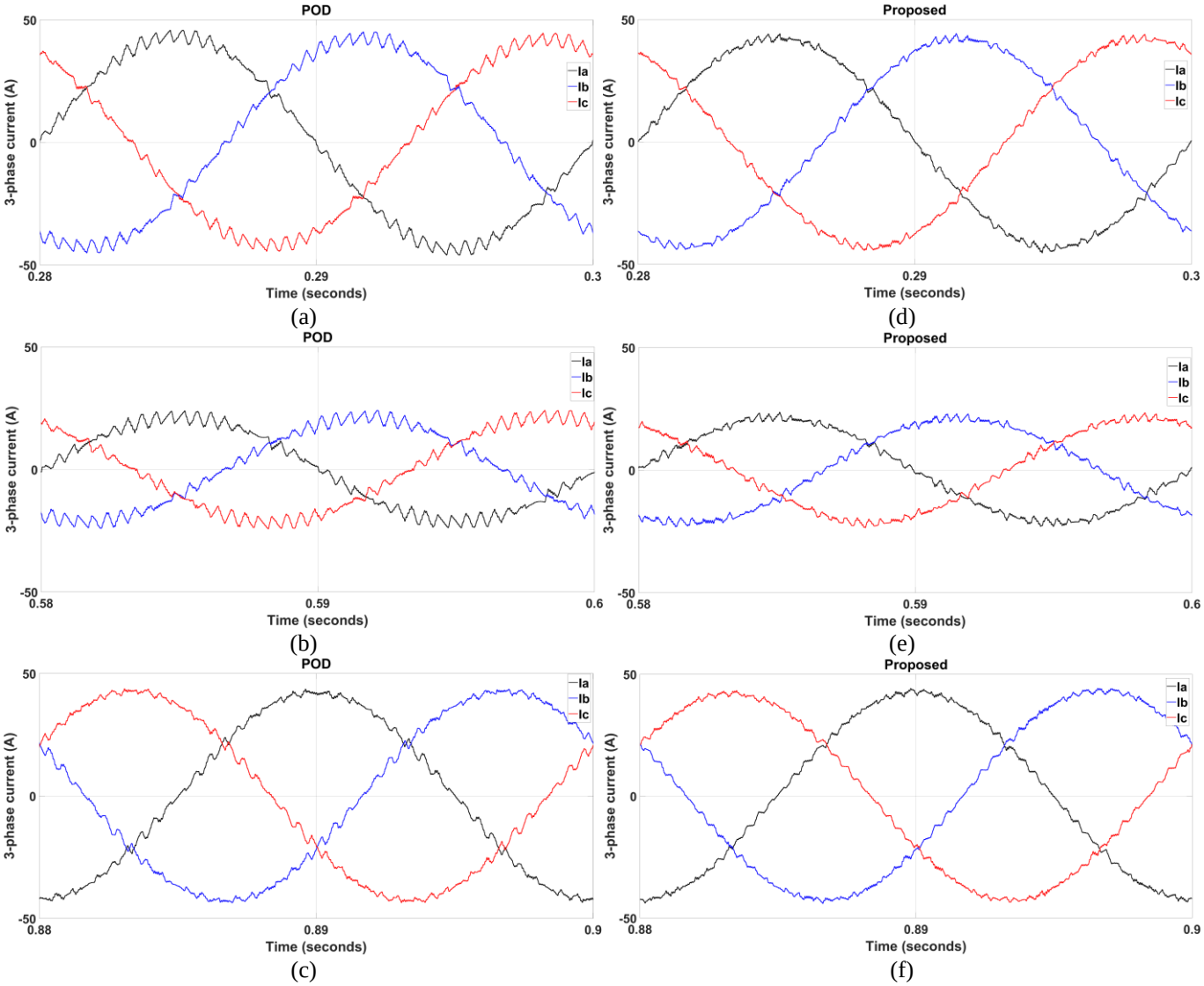

Fig. 10. Current waveforms magnified: (a)-(c) – of POD method and (d)-(f) – proposed method.

Especially in the second interval, the phase current ripple of the POD method in Fig. 10(b) is significantly higher than that of the proposed method in Fig. 10(e). The spectra and THD of phase currents have also been presented in Fig. 11 and taken in the last fundamental period of the intervals of time.

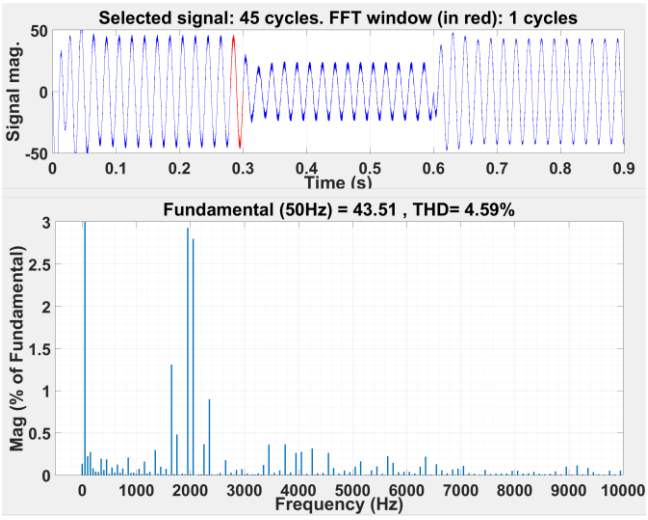

(a) Taken at 0.28 s

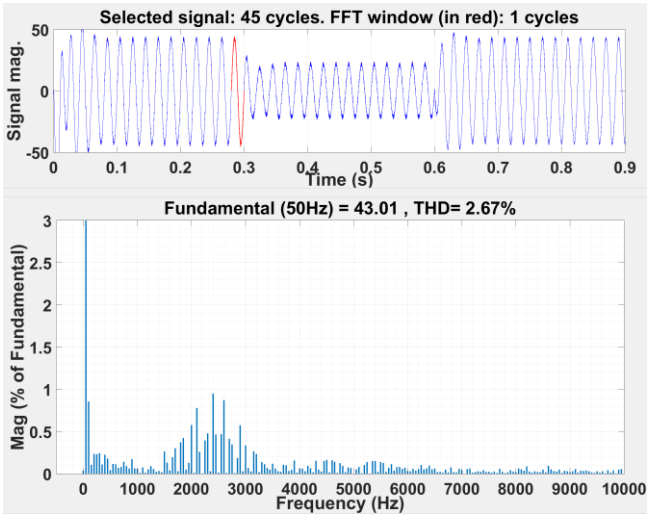

(d) Taken at 0.28 s

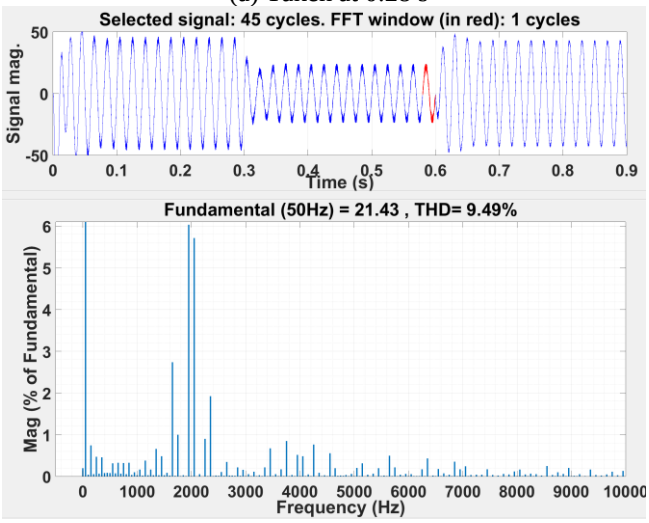

(b) Taken at 0.58 s

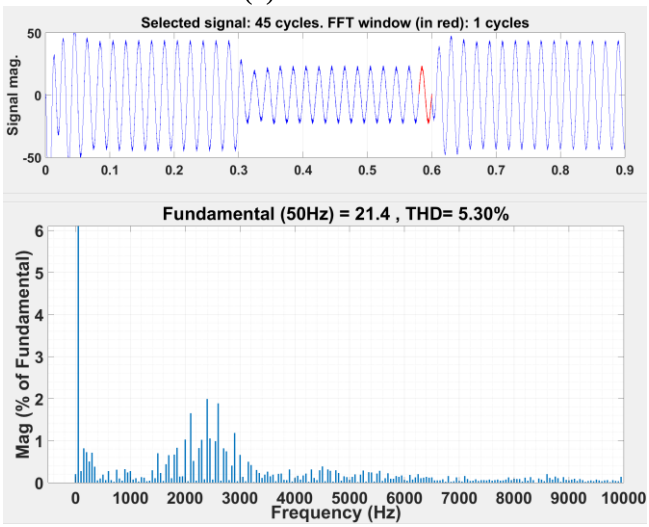

(e) Taken at 0.58 s

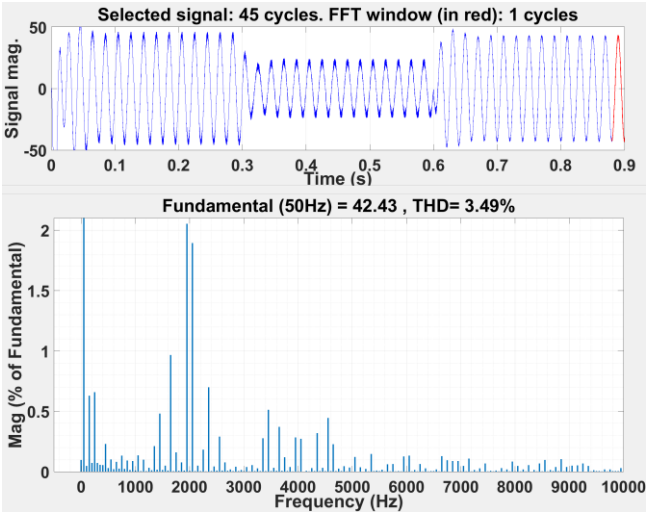

(c) Taken at 0.88 s

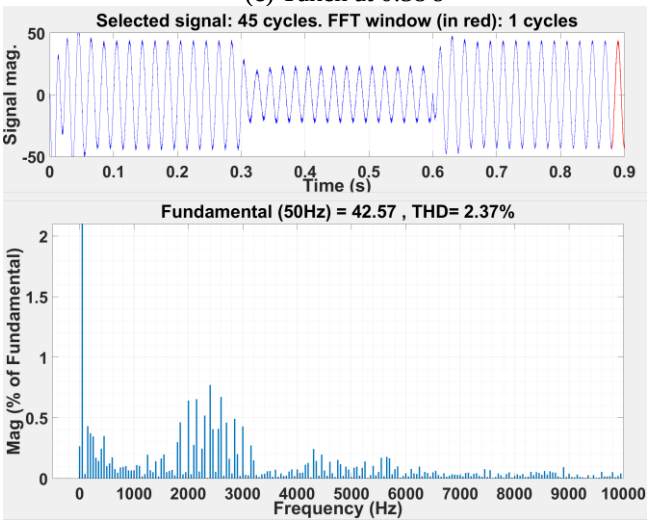

(f) Taken at 0.88 s

Fig. 11. Phase current THD and spectra of: (a)-(c) – POD method and (d)-(f) - proposed method.

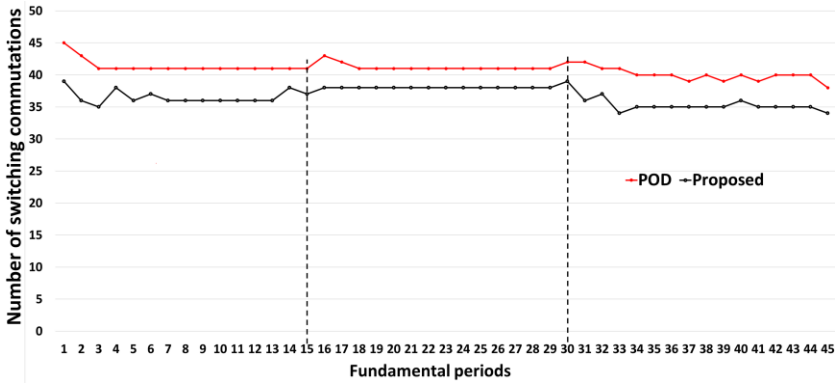

Fig. 12. The number of switching commutations of the two methods

In the first interval, the current THD value of the POD method in Fig. 11(a) is 4.59% whilst that of the proposed method in Fig. 11(d) is 2.67%. In addition, the highest magnitude of individual harmonic in Fig. 11(a) is up to 2.9% and exceeds the limit (1%) while that of the proposed method in Fig. 11(d) is lower 1%. Similarly, in the second interval, the current THD value in Fig. 11(b) is 9.49% is also higher than that of the proposed method in Fig. 11(e) as 5.3%. In the third interval, the current THD value of the proposed method in Fig. 11(f) is only 2.37%. On the contrary, the THD value in Fig. 11(c) is up to 3.49% and greater than that of the proposed method.

Moreover, the highest magnitudes of individual harmonics in Figs. 11(b)-(c) are 6% and 2.05% respectively. While those in Figs. 11(e)-(f) of the proposed method are only 2% and 0.8% respectively. This has proved that the modulation using the variable frequency carriers can spread the current spectrum over a wide range and reduce acoustic noise. This also is suitable for devices applied in communication and military.

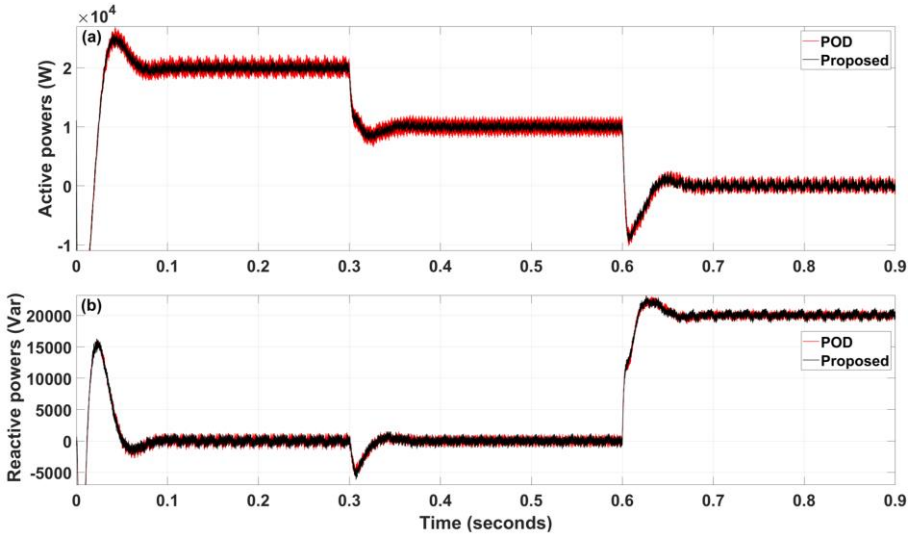

Fig. 13. Power responses

In addition, the surveyed results in Fig. 12 have shown that the proposed method can also significantly reduce the number of switching commutations. In 45 fundamental periods surveyed in Fig. 12 corresponding to the three intervals, 0-0.9 (s), the number of switching commutations of the proposed method is always lower than that of the method using POD.

Thus, the method using variable frequency carriers helps reduce not only the current harmonics but also the number of switching commutations of inverter.

The lower current harmonic of the method using variable frequency carriers can also help reduce the power ripple in Fig. 13 of the proposed method lower than that of the method using POD.

5. Conclusion

Based on the analysis of the influences of the carrier in the modulation of inverters, this paper has proposed a method using the variable frequency carriers to modulate the grid-connected cascaded multilevel 3-phase inverters. The carrier frequency varies according to the magnitude of the control signal. The advantage of this method is the ability to spread the spectrum over a wide range and help significantly reduce the individual harmonics of inverters. In addition, the proposed method also helps reduce the CMV magnitude as $V_{dc}/3$ similar to that of the POD modulation. This method helps reduce not only the THD values but also the number of switching commutations compared with the POD method.

The effectiveness of the proposed method has been validated when comparing the surveyed results of the proposed method with those of the method using the POD modulation based on the system of grid-connected cascaded 5-level 3-phase inverter.

Acknowledgements

This work belongs to the project in 2023 funded by Ho Chi Minh City University of Technology and Education, Vietnam.

References

[1] S. Mehta and V. Puri, "A review of different multi-level inverter topologies for grid integration of solar photovoltaic system," *Renew. Energy Focus*, vol. 43, pp. 263–276, Dec. 2022, doi: 10.1016/J.REF.2022.10.002.
[2] G. Griva, S. Musumeci, R. Bojoi, P. Zito, S. Bifaretti, and A. Lampasi, "Cascaded multilevel inverter for vertical stabilization and radial control power supplies," *Fusion Eng. Des.*, vol. 189, p. 113473, Apr. 2023, doi: 10.1016/J.FUSENGDES.2023.113473.
[3] A. Mittal, K. Janardhan, and A. Ojha, "Multilevel inverter based Grid Connected Solar Photovoltaic System with Power Flow Control," *2021 Int. Conf. Sustain. Energy Futur. Electr. Transp. SeFet 2021*, pp. 5–10, 2021, doi: 10.1109/SeFet48154.2021.9375753.
[4] W. Rahmouni, G. Bachir, and M. Aillerie, "A new control strategy for harmonic reduction in photovoltaic inverters inspired by the autonomous nervous system," *J. Electr. Eng.*, vol. 73, no. 5, pp. 310–317, 2022, doi: 10.2478/jee-2022-0041.
[5] N. T. Mbungu, R. M. Naidoo, R. C. Bansal, M. W. Siti, and D. H. Tungadio, "An overview of renewable energy resources and grid integration for commercial building applications," *J. Energy Storage*, vol. 29, p. 101385, Jun. 2020, doi: 10.1016/J.EST.2020.101385.
[6] J. Stöttner, A. Rauscher, and C. Endisch, "Pareto optimization of multilevel inverter structures regarding the DC magnitude, switching frequency and switching angles," *Int. J. Electr. Power Energy Syst.*, vol. 142, p. 108259, Nov. 2022, doi: 10.1016/J.IJEPES.2022.108259.
[7] C. Dhanamjayulu, P. Sanjeevikumar, and S. M. Muyeen, "A structural overview on transformer and transformer-less multilevel inverters for renewable energy applications," *Energy Reports*, vol. 8, pp. 10299–10333, Nov. 2022, doi: 10.1016/J.EGYR.2022.07.166.
[8] C. C. Hou, C. C. Shih, P. T. Cheng, and A. M. Hava, "Common-mode voltage reduction pulsewidth modulation techniques for three-phase grid-connected converters," *IEEE Trans. Power Electron.*, vol. 28, no. 4, pp. 1971–1979, 2013, doi: 10.1109/TPEL.2012.2196712.
[9] C. Mai-Van, S. Duong-Minh, D. Tran-Huu, B. Binh-Pho, and P. Vu, "An improved method of model predictive current control for multilevel cascaded H-bridge inverters," *J. Electr. Eng.*, vol. 72, no. 1, pp. 1–11, 2021, doi: 10.2478/jee-2021-0001.
[10] B. B. Pho, C. Mai-Van, M. T. Trong, and P. Vu, "Model predictive control for distributed MPPT algorithm of cascaded H-bridge multilevel grid-connected PV inverters," *J. Electr. Eng.*, vol. 73, no. 4, pp. 305–309, 2022, doi: 10.2478/jee-2022-0040.
[11] C. Wang, Y. He, Y. Wang, and J. Liu, "Research of the equivalent relationship between the space vector and the triangular carrier-based PWM modulation strategies in the flying capacitor multilevel inverters," *Int. J. Electron.*, vol. 106, no. 3, pp. 395–414, 2019, doi: 10.1080/00207217.2018.1540061.
[12] B. Li, R. Yang, D. Xu, G. Wang, W. Wang, and D. Xu, "Analysis of the phase-shifted carrier modulation for modular multilevel converters," *IEEE Trans. Power Electron.*, vol. 30, no. 1, pp. 297–310, 2015, doi: 10.1109/TPEL.2014.2299802.
[13] G. S. Ariya Thankachy and G. Shiny, "Phase shifted carrier modulation technique for modular multilevel inverter," *IEEE Int. Conf. Power Electron. Drives Energy Syst. PEDES 2016*, vol. 2016-Janua, pp. 1–6, 2017, doi: 10.1109/PEDES.2016.7914340.
[14] M. Jamil, "Carrier-based modulation strategies for a neutral point clamped inverter," *Int. J. Electron.*, vol. 95, no. 12, pp. 1293–1303, 2008, doi: 10.1080/00207210802524294.
[15] A. Alexander Stonier, "Design and development of high performance solar photovoltaic inverter with advanced modulation techniques to improve power quality," *Int. J. Electron.*, vol. 104, no. 2, pp. 174–189, 2017, doi: 10.1080/00207217.2016.1196746.
[16] M. Salem, A. Richelli, K. Yahya, M. N. Hamidi, T. Z. Ang, and I. Alhamrouni, "A Comprehensive Review on Multilevel Inverters for Grid-Tied System Applications," *Energies*, vol. 15, no. 17, 2022, doi: 10.3390/en15176315.
[17] R. Mahalakshmi and K. C. S. Thampatty, "Grid Connected Multilevel Inverter for Renewable Energy Applications," *Procedia Technol.*, vol. 21, pp. 636–642, 2015, doi: 10.1016/j.protcy.2015.10.076.
[18] Q.-T. Tran, A. V. Truong, and P. M. Le, "Reduction of harmonics in grid-connected inverters using variable switching frequency," *Int. J. Electr. Power Energy Syst.*, vol. 82, pp. 242–251, 2016, doi: 10.1016/j.ijepes.2016.03.027.
[19] V. Q. Nguyen, T. Q. Tho, and H. N. Duong, "Stator-flux-oriented control for three- phase induction motors using sliding mode control," *J. Electr. Syst.*, vol. 16, no. 2, pp. 171–184, 2020.

Received 9 April 2023